DOI:
10.1016/j.jacep.2017.01.018

Document Version
Peer reviewed version

JACC: CLINICAL ELECTROPHYSIOLOGY VOL. ■, NO. ■, 2017

ISSN 2405-500X
http://dx.doi.org/10.1016/j.jacep.2017.01.018

Real-Time X-MRI-Guided Left Ventricular Lead Implantation for Targeted Delivery of Cardiac Resynchronization Therapy

Jonathan M. Behar, MBBS, BSc,[a] Peter Mountney, PhD,[b] Daniel Toth, MSc,[a,c] Sabrina Reiml, BSc,[d] Maria Panayiotou, PhD,[a] Alexander Brost, PhD,[d] Bernhard Fahn, MSc, PhD,[d] Rashed Karim, PhD,[a] Simon Claridge, LLB, MBBS,[a] Tom Jackson, MBBS,[a] Ben Sieniewicz, MBBS,[a] Nik Patel, MBBS,[a] Mark O'Neill, MD, DPhil,[a] Reza Razavi, MD,[a] Kawal Rhode, PhD,[a] Christopher Aldo Rinaldi, MD[a]

ABSTRACT

OBJECTIVES This study sought to test the feasibility of a purpose-built, integrated software platform to process, analyze, and overlay cardiac magnetic resonance (CMR) data in real time within a cardiac catheter laboratory and magnetic resonance imaging scanner in the same facility with the ability to transfer patients from one to the other (X-MRI) environment to guide left ventricular (LV) lead implantation.

BACKGROUND Suboptimal LV lead position is a major determinant of poor cardiac resynchronization therapy (CRT) response, and the optimal site is highly patient specific. Pacing myocardial scar is associated with poorer outcomes; conversely, targeting latest mechanical activation (LMA) may improve them.

METHODS Fourteen patients (age 74 ± 5.1 years; New York Heart Association functional class: 2.7 ± 0.4; 86% ischemic with ejection fraction 27 ± 7.6%; QRSd: 157 ± 19 ms) underwent CMR followed by immediate CRT implantation using derived scar and dyssynchrony data, overlaid onto fluoroscopy in an X-MRI suite. Rapid LV segmentation enabled detailed scar quantification, identification of LMA segments, and selection of myocardial targets. At coronary venography, the CMR-derived 3-dimensional shell was fused, enabling identification of viable venous targets subtended by target segments for LV lead placement.

RESULTS The platform was successful in all 14 patients, of whom 10 (71%) were paced in pre-procedurally defined target segments. Pacing in CMR-defined target segments (out of scar) showed a significant decrease in the LV capture threshold (mean difference: 2.4 [1.5 to 3.2]; $p < 0.001$) and shorter paced QRS duration (mean difference: 25 [15 to 34]; $p < 0.001$) compared with pacing in areas of CMR determined scar. In 5 (36%) patients with extensive scar in the posterolateral wall, CMR guidance enabled successful lead delivery in an alternative anatomically favorable site. Radiation dose and implant times were similar to historical controls ($p = NS$).

CONCLUSIONS Real-time CMR-guided LV lead placement is feasible and achievable in a single clinical setting and may prove helpful to preferentially select sites for LV lead placement. (J Am Coll Cardiol EP 2017;■:■–■) © 2017 The Authors. Published by Elsevier on behalf of the American College of Cardiology Foundation. This is an open access article under the CC BY license (http://creativecommons.org/licenses/by/4.0/).

From the [a]Department of Imaging Sciences and Biomedical Engineering, King's College London, & Guy's and St Thomas' Hospital, London, United Kingdom; [b]Medical Imaging Technologies, Siemens Healthineers, Princeton, New Jersey; [c]Siemens Healthineers, Frimley, Camberley, United Kingdom; and [d]Siemens Healthcare GmbH, Erlangen, Germany. This research was supported from Innovate UK (32684-234174), National Institute for Health Research Biomedical Research Centre based at Guy's and St Thomas NHS Foundation Trust and Kings College London. Dr. Behar acknowledges support from the Rosetrees Trust. Dr. Claridge has received research fellowship funding from St Jude Medical Ltd. Dr. Jackson has received research fellowship funding from Medtronic Inc. Dr. Rinaldi is consultant to St Jude Medical Ltd., Medtronic, and Spectranetics; and receives research funding from St. Jude Medical and Medtronic, Boston Scientific, and Livanova. Drs. Mountney and Toth are employees of Siemens Healthcare Ltd., Frimley, United Kingdom. Ms. Reiml, Mr. Fahn, and Dr. Brost are employees of Siemens Healthcare GmbH, Erlangen, Germany. Drs Rhode and Rinaldi contributed equally to this work and are joint senior authors on this paper.

Manuscript received September 26, 2016; revised manuscript received January 23, 2017, accepted January 27, 2017.

ABBREVIATIONS AND ACRONYMS

CMR = cardiac magnetic resonance

CRT = cardiac resynchronization therapy

CS = coronary sinus

CT = computed tomography

3D = 3-dimensional

FA = flip angle

LGE = late gadolinium enhancement

LV = left ventricular

QLV = first ventricular depolarization (earliest onset QRS duration on surface 12-lead electrocardiogram) to the nadir signal on the LV lead electrogram

TE = echo time

TR = repetition time

X-MRI = cardiac catheter laboratory and MRI scanner in the same facility with the ability to transfer patients from one to the other

Cardiac resynchronization therapy (CRT) is a highly efficacious treatment for symptomatic patients with heart failure, severe left ventricular (LV) dysfunction, and broad QRS duration (1,2). Despite 2 decades of delivering biventricular pacing for selected patients with heart failure, 30% to 50% fail to undergo LV remodeling (3), with most implanters using empirical placement of the LV lead on the posterolateral wall. However, the optimal site for LV stimulation is highly patient specific (4) and suboptimal lead position is a major determinant of poor response (5). LV lead positioning in or near areas of myocardial fibrosis is associated with poorer outcomes (6–8). Furthermore, targeting LV myocardial segments with latest mechanical activation using speckle tracking echocardiography has demonstrated utility in improving CRT outcomes in single-center randomized studies (9,10). Echocardiography, however, is a highly user-dependent imaging modality and the reproducibility of dyssynchrony metrics is limited (11,12). Cardiac magnetic resonance (CMR) imaging has recently emerged as a highly valuable modality providing unparalleled image quality and information on etiology for patients with heart failure (6); furthermore, it can delineate the location and burden of myocardial scar through late gadolinium enhancement sequences (13) and provide valuable data on mechanical dyssynchrony (14) and LV contraction patterns (15), both of which can inform appropriate placement of the LV lead. We have previously demonstrated the ability to overlay CMR-derived anatomy, scar, and dyssynchrony data onto fluoroscopy for guiding the placement of the LV lead (16,17). This resulted in improved acute response and chronic echocardiographic response above the rates in a standard nonguided approach. However, the large quantity of data, associated lengthy computational processing time, and highly manual process, as well as software limitations at that time meant CMR scans were performed at least 2 weeks before the implant.

The ability to process and display such information in real time would represent a significant advance in the ability to use CMR guidance. In this paper, we report the first demonstration of a real-time, purpose-built user interface in a hybrid cardiac catheter laboratory and magnetic resonance imaging scanner in the same facility with the ability to transfer patients from one to the other (X-MRI) facility to enable the processing, analysis and fusion of CMR-derived data to guide the implanting physician in optimizing the deployment of an LV lead for CRT delivery. Using this technique, the implanting physician can use contemporaneous gold standard myocardial imaging to avoid regions of scar while targeting late activating segments, thereby permitting imaging-guided LV lead implantation in a single procedure.

METHODS

This study complied with the Declaration of Helsinki and the protocol was approved by the local ethics committee. Informed written consent was obtained from each patient. A comprehensive CRT preassessment included New York Heart Association class, Minnesota Living with Heart Failure Questionnaire score, 6-min walk distance, peak oxygen uptake on cardiopulmonary exercise testing, and echocardiographic assessment of LV systolic function with 2-dimensional and 3-dimensional (3D) datasets. Patients with a contraindication to CMR or significant renal impairment (estimated glomerular filtration rate: <30 ml/min/1.73 m^2) were excluded. Patients fulfilling standard CRT criteria (New York Heart Association functional class II-IV drug refractory heart failure, LV ejection fraction $<35\%$, and QRS >120 ms) were included in the study.

INTEGRATED SOFTWARE MODULE. A custom-made software platform developed by the Department of Imaging Sciences & Biomedical Engineering and Siemens Healthineers was integrated in the X-MRI facility incorporating a Magnetom Aera 1.5T MRI scanner and adjacent Artis Q biplane Angiography system (Siemens Magnetom Artis Combi Suite, Siemens Healthcare GmbH, Erlangen, Germany).

The platform was installed on a dedicated prototype workstation connected to the biplane x-ray system. It was designed for fast, automated data processing to enable information to be extracted from MRI and visualized in the time it takes to transfer the patient from the MRI to angiography suite to minimize any disruption. The platform includes automatic intra- and inter-MRI protocol slice registration, automatic LV segmentation, semiautomatic scar segmentation and metrics for mechanical dyssynchrony, scar distribution, burden, and transmurality. After each automated task, the clinician is given the opportunity to verify and manually adjust the results.

PATIENT FLOW AND CRT IMPLANT. Respiratory and cardiac-gated CMR images were acquired. Two-, 3-, and 4-chamber and multiple slice short-axis balanced steady-state free-precession images were acquired

during breath hold (repetition time [TR]: 2.4 ms; echo time [TE]: 1.2 ms; flip angle [FA]: 52°; acquired spatial resolution: 1.3 to 1.8 × 1.9 to 2.8 mm; bandwidth: 930 Hz/pixel; 6-mm slice thickness [long], 8-mm slice thickness [short]) using an 18-channel body coil and a 24-channel spine coil. Late gadolinium enhancement (LGE) sequences in the same views (TR: 2.4 ms; TE: 1.2 ms; FA: 45°; acquired spatial resolution: 1.10 × 2.5 mm; bandwidth: 780 Hz/pixel; 8-mm slice thickness with 2-mm gaps) was performed 10 to 15 min following administration of 0.2 mmol/kg Gadovist (Bayer Healthcare, Berlin, Germany) using conventional inversion recovery techniques to identify areas of myocardial fibrosis (13). Following completion of the scan, the patient was transferred directly to the catheter laboratory (Combi Dockable Table, Siemens Healthcare GmbH) and prepared for CRT implantation, which began immediately after the scan. Simultaneously, the CMR data were uploaded, processed, and analyzed on the prototype platform using the following steps (Figure 1):

1. LV epicardial and endocardial automated segmentation with manual adjustment where necessary.
2. Registration of cine and LGE sequences.
3. Delineation of myocardial fibrosis.
4. Review of location, burden, and transmurality of myocardial fibrosis on a 16-segment American Heart Association (AHA) bull's-eye plot and the associated regional dyssynchrony curves to select optimal target myocardial segments for LV delivery.

FIGURE 1 Patient and Data Processing Workflow

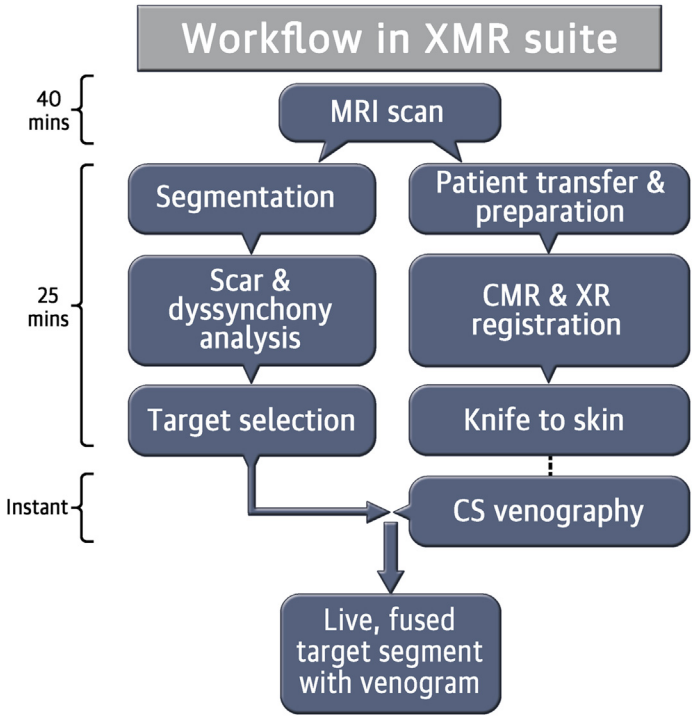

CMR = cardiac magnetic resonance; CS = coronary sinus; MRI = magnetic resonance imaging; XMR = cardiac catheter laboratory and MR scanner in the same facility with the ability to transfer patients from one to the other; XR = x-ray.

LV SEGMENTATION AND MECHANICAL DYSSYNCHRONY COMPUTATION. The automated segmentation algorithm uses a combination of landmark detection and discrimination between the myocardium and blood pool in each short- and long-axis slice to create a 3D mesh model. The algorithms on which this is based have been previously described (18). Epicardial and endocardial segmented contours are divided into basal, mid, and apical segments. Identification of the right ventricular insertion points further divides segments in line with AHA-recommended nomenclature. Segmental endocardial volumes are computed by multiplication of segmental area by slice thickness. Each AHA regional volume is calculated throughout the cardiac cycle (25 to 30 phases) to produce volume vs. time curves. Time to minimum endocardial volume is assumed to be the time to peak strain and expressed as a fraction of the cardiac cycle length, denoted by a colored dot on each segmental curve (lower left panel, Figure 2). The mechanical activation curves are generated automatically after the user confirms the segmentation of epicardial and endocardial shells from the short-axis cine sequences and has reviewed these segmentations tracking over the cardiac cycle length.

MYOCARDIAL FIBROSIS IDENTIFICATION. The cine short-axis sequences are first registered to the LGE sequences to translate myocardial fibrosis to the LV mesh. Subsequently, an automated algorithm computes and highlights regions of scar (LGE) after the user identifies a region of healthy tissue; LGE was defined as 2 standard deviations from the mean gray level. Users can adjust and manually add or remove areas of fibrosis while reviewing each slice.

DATA REVIEW AND TARGET SELECTION. Following the steps described previously, a guidance display is shown from which physicians select target segments according to the principle of avoiding myocardial scar and targeting areas of mechanical dyssynchrony (latest time to peak contraction) in line with our previously published work (15) (Figure 2).

FIGURE 2 Prototype Display

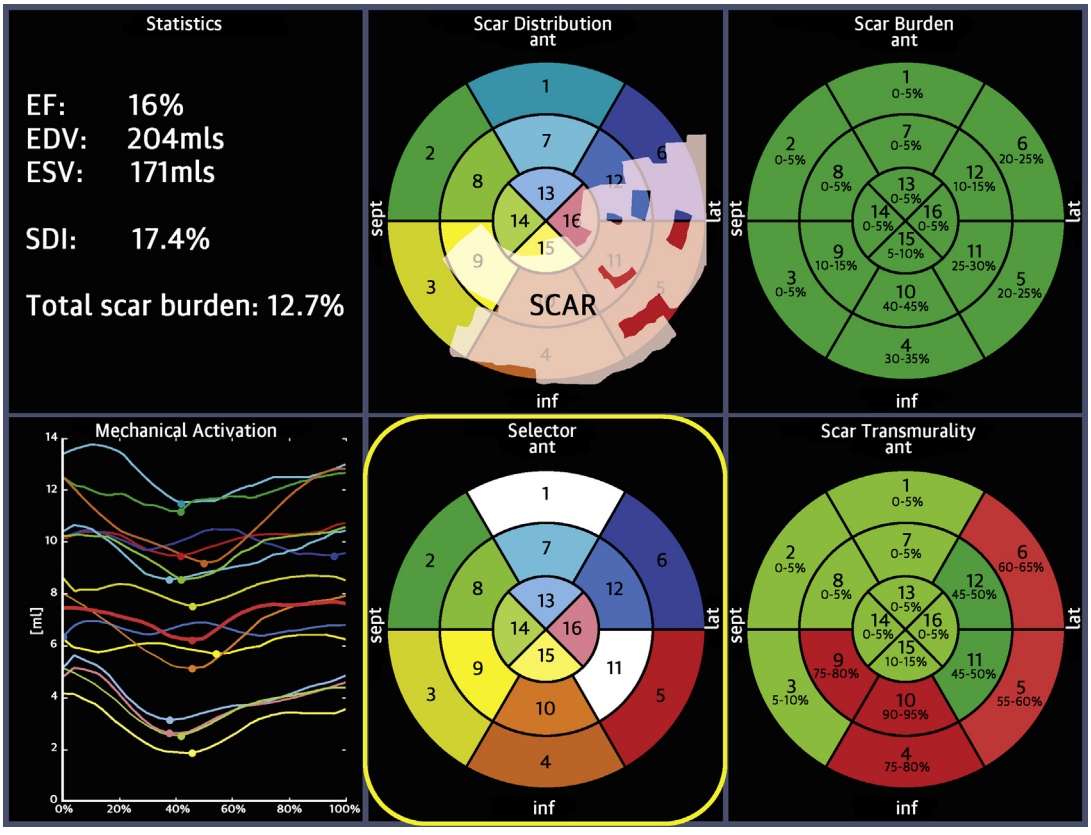

This display screen is seen following the processing of the CMR dataset and is mimicked on the large screen in the catheter laboratory. Total scar burden calculated as a mean of all myocardial segments. **(Top middle)** Scar distribution denoted in **gray** upon an American Heart Association 16-segment model. **(Top right)** Scar burden (% scar per myocardial segment volume), displayed in 5% ranges. **(Bottom right)** Scar transmurality demonstrating the mean transmurality from endocardium to epicardium. Those segments >50% transmural myocardial fibrosis are also denoted in **red**. **(Bottom left)** Mechanical activation curves for the 16 segments, corresponding to the colors shown in the **middle panels**. Endocardial tracking of the left ventricle provides absolute changes in the volume per segment (ml, y axis) over the cardiac cycle (0% end diastole, 30% to 50% end systole, 100% end diastole). Because these are absolute volume changes, the apical segments are always at the bottom because they have a smaller start and end volume. When the user hovers over a segment in the top middle panel, the associated volume time curve appears in bold; in this case, the target posterolateral segment is shown. **(Bottom middle)** Target selection panel. Upon reviewing the scar location, burden, transmurality, and mechanical activation curves, target segments are chosen (seen here in **white**; basal anterior, mid-posterolateral). EDV = end-diastolic volume; EF = ejection fraction; ESV = end-systolic volume; SDI = systolic dyssynchrony using endocardial tracking of CMR cine images in short and long axis; other abbreviations as in Figure 1.

Where there was extensive myocardial fibrosis, segments with the smallest scar burden and transmurality were selected. Septal segments were excluded because epicardial LV stimulation in this region does not achieve effective resynchronization. Where scar was absent, target segments with the most delayed time to minimum volume were chosen. Segments with a minimal change in volume and therefore reduced endocardial strain were excluded for selection on the basis of likely nonviability and previously published work linking LV placement in such regions with poor CRT outcomes (19).

IMAGE GUIDANCE. A 3D model derived from CMR was coregistered with x-ray images using multimodality imaging markers placed on the left side of the chest overlying the heart (Beekley Medical, Bristol, Connecticut) and visible on both CMR and x-ray images. A 3D spoiled gradient echo, time-resolved angiography with interleaved stochastic trajectories sequence was used to identify the adhesive markers (TR: 2.56; TE: 0.9; FA: 30°; slice thickness: 1.3 mm; acquired spatial resolution: 1.3 × 1.9 mm) on CMR and these were registered to biplane fluoroscopic images using the platform. Six

degrees of freedom, translation, and rotation ensured the accuracy of the registration in orthogonal planes. Following this process, the CMR-derived 3D model is registered to the x-ray coordinate system; subsequent x-ray acquisitions during the case are displayed with instantaneous overlay of the correctly oriented 3D model (Figure 3).

Steps 1 through 4 were completed while the patient was being prepared for the implantation. Following coronary sinus (CS) cannulation, occlusive venography in right anterior oblique, anteroposterior, and left anterior oblique projections were obtained and instantaneously fused with the CMR-derived 3D model of the patient's left ventricle (both epicardium and endocardium), as shown in Figure 4. The number and anatomical location of viable epicardial coronary venous targets was immediately visualized on the AHA 16-segment plot. Scar location and target selection meshes could be selectively highlighted to guide LV lead positioning (Figure 4). LV lead deployment was performed in the standard fashion aiming to place the lead in the targeted segment when CS anatomy was favorable and the target threshold was <2.5 V at 0.5 ms with no phrenic nerve stimulation at 10 V. A quadripolar LV lead was used in all cases.

Before finalizing the LV lead position, to further validate the guidance system in relation to scar and local electrical activation (QLV), all epicardial veins (able to receive an LV lead) were tested. Multiple vector configurations were attempted along each vein where possible and the QLV (ms), capture thresholds (V), and paced QRS (ms) were measured.

STATISTICS. A test for normality (Shapiro-Wilk) was performed for each variable. Continuous variables with a Gaussian distribution were described using mean ± standard deviation; those with non-normal distribution were described with median, interquartile range. Categorical data were described by an absolute number of occurrences and associated frequency (%). Because of different numbers of multiple measurements per patient, an ordinary Student *t* test would not be appropriate and a mixed-effect model was performed. Results were considered statistically significant at $p < 0.05$. Analysis was performed on PASW Statistics 22 (SPSS Inc., Chicago, Illinois) and Stata (StataCorp, 2014, Statistical Software, College Station, Texas) for the mixed linear model. In the text capture, thresholds are described to 1 decimal place and QLV/biventricular-paced QRS described to no decimal places, for clinical relevance.

RESULTS

Fourteen patients underwent real-time X-MRI-guided lead implantation. Patients were age 74 ± 5.1 years and all were successfully implanted with a new CRT device (13 [93%]). Twelve (86%) patients had subendocardial myocardial fibrosis; 2 patients had

FIGURE 3 **Image Panel of Workflow**

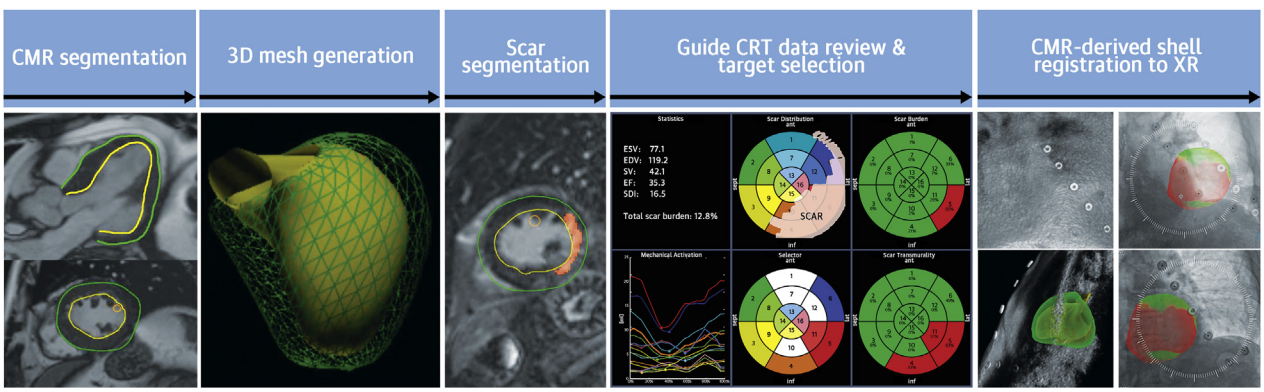

The first step involves the automated segmentation and manual adjustment of the epicardial and endocardial slices to generate a 3-dimensional (3D) mesh. Endocardial wall motion is tracked over the cardiac cycle to generate volume vs. time curves for the 16 segments. Following registration of the cine to late gadolinium enhancement sequences, areas of myocardial fibrosis are identified and both scar and dyssynchrony data are reviewed and targets selected. The 3D shell is then registered to the x-ray (XR) once the patient is on the catheter laboratory table using fiducial markers, which show up **white** (from the CMR sequences) and **gray** with a central dark dot (lead ball-bearing) from the x-ray. Vertical and horizontal translation using biplane fluoroscopy is used, in addition to rotation about the x, y, and z axes to line up the markers as demonstrated on the **right hand panel**. Following this process, the CMR-derived 3D model is registered to the XR system and every fluoroscopic cine demonstrates the epicardial and endocardial shell overlaid in the correct orientation.

FIGURE 4 **CMR-Derived Image Overlay With Target Segment Selection**

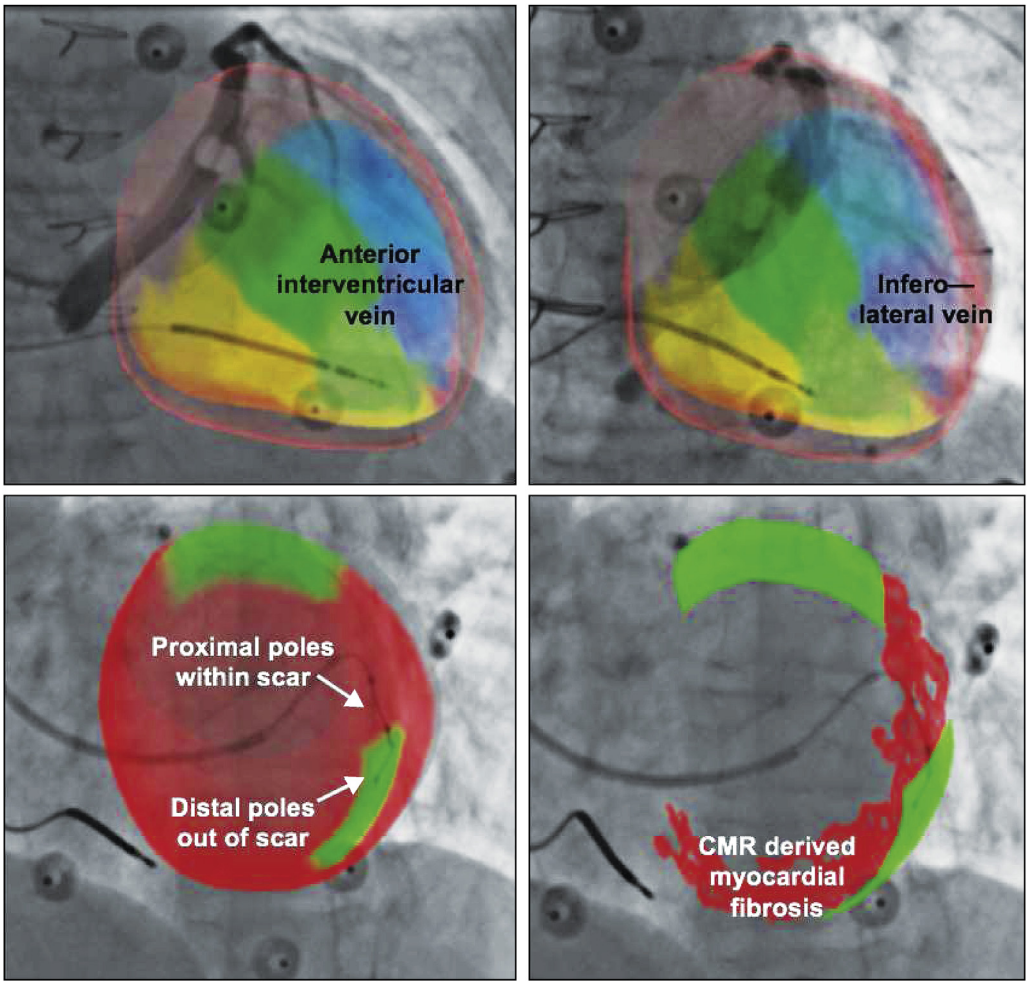

(Top left) Anteroposterior venogram with overlay of CMR-derived epicardial/endocardial shell with 16-segment American Heart Association model showing an anterior interventricular vein. The 3D CMR-derived shell has the same colors as displayed in the guidance platform as shown in Figures 2 and 3. Posteroseptal, anteroseptal, and anterior segments are colored in **yellow, green, and blue**, respectively. **(Top right)** left anterior oblique (LAO) 20 venogram with automated rotation and alignment of the 16-segment model with the x-ray. Posterolateral veins are demonstrated. **(Bottom left)** LAO 40 projection. Positioning of a quadripolar left ventricular lead into a preselected target segment **(green)**. **(Bottom right)** LAO 40 projection, alternate view with CMR-derived scar distribution **(red)**. Attempted positioning and pacing using left ventricular poles out of regions of scar.

nonischemic cardiomyopathy (Table 1). Total procedural time including CMR (45 ± 6 min), data processing and patient transfer/preparation (25 ± 8 min), and CRT implant (115 ± 33 min) was 185 ± 35 min. Radiation dose area product was similar to recent historical controls (conventional CRT implants): 1,893 ± 1,965 cGycm^{2}vs. 1,582 ± 2,122 cGycm^2, p = 0.72. There were no post-operative complications and no adverse effect on renal function despite use of intravenous gadolinium and iodinated contrast within a short space of time. Of note, patients in this study had all accessible coronary veins tested for LV lead implantation compared with the historical controls, in which this is not routine practice.

A mean of 3.6 ± 1 epicardial coronary veins were visible at venography (total: 51), of which 2.4 ± 0.8 (total: 33) were judged to be viable targets for LV lead deployment on the basis of anatomical location and vessel caliber. Biventricular stimulation was performed from these sites. A total of 56 data points were acquired across 14 patients (range: 1 to 10) (Online Table 1) in all possible epicardial veins.

TABLE 1 Demographic Data

Age (yrs)	74 ± 5.1
NYHA functional class	2.7 ± 0.4
Left ventricular ejection fraction (%)	27 ± 7.6
QRS duration (ms)	157 ± 19
Left bundle branch block	12 (86%)
MLHFQ score (points)	27 ± 18
6-min walking distance (m)	356 ± 72
NT-pro BNP (ng/l)	3,429 ± 3,136
Sinus rhythm	11 (79%)
3D Systolic dyssynchrony index (%)	15.0 ± 7.4
Peak VO_2 (ml/min/kg)	14.8 ± 5.4
VE/VCO_2 slope	38 ± 14
Myocardial fibrosis burden (% total volume, AHA 16 segment)*	11.9 ± 6.4
On beta blocker	79%
On ACE inhibitor	93%
On MRA	50%
On antiplatelet therapy	64%

Values are mean ± SD, n (%), or %. *Scar burden calculated using prototype platform.

ACE = angiotensin-converting enzyme; BNP = B-type natriuretic peptide; 3D = 3-dimensional; MLHFQ = Minnesota Living with Heart Failure Questionnaire; MRA = magnetic resonance angiography; NYHA = New York Heart Association; peak VO_2 = peak oxygen uptake on cardiopulmonary exercise testing.

In some cases, multiple data points were collected along veins using different vectors from the multipolar LV lead. In 10 of 14 (71%) patients, LV lead implantation was achieved in the CMR-defined target segments based upon avoiding scar and targeting mechanical dyssynchrony (e.g., **Figure 5**). The 4 remaining patients were paced in/adjacent to scar because of a lack of coronary venous anatomy to the target segment. Pacing in CMR-defined target segments (out of scar) showed a statistically decreased mean in the LV lead capture threshold (mean difference: 2.4 [1.5 to 3.2]; $p < 0.001$) and shorter biventricular paced QRS duration (mean difference: 25 [15 to 34]; $p < 0.001$) compared with areas in areas of scar as defined by the CMR overlay. There was no significant difference for QLV (mean difference: 8 [-9 to 24]; $p = 0.35$) (**Table 2**). Six patients had anterior/anteroseptal scar, 5 patients had posterolateral scar, 1 patient had anterolateral scar, and 2 patients had no scar. In cases where the only viable veins were in or adjacent to scar (particularly those with posterolateral scar), image overlay facilitated positioning of the poles on the multipolar LV lead away from scar as depicted in **Figure 5**.

DISCUSSION

This study demonstrates for the first time the safety and feasibility of real-time CMR-defined scar and dyssynchrony to successfully guide LV lead implantation for CRT delivery in a single procedure. Furthermore, pacing within CMR-defined segments (out of scar) showed more favorable electrical properties (lower LV capture thresholds and shorter BV-paced QRS duration) as compared with regions of scar, confirming validity to this approach.

IMAGE-GUIDED CRT: COMPARISON WITH PREVIOUS STUDIES. Two randomized studies have previously shown the benefit of targeted LV lead placement over an empirical approach. The TARGET (Targeted Left Ventricular Lead Placement to Guide Cardiac Resynchronization Therapy) (8) and STARTER (Speckle Tracking Assisted Resynchronization Therapy for Electrode Region) (9) studies showed significant improvements in LV remodelling by using 2-dimensional speckle tracking echocardiography to define and target late activating segments. Cardiac imaging was however, performed at a separate sitting prior to implantation and the images were not fused with fluoroscopy. In 11% of the patients recruited to TARGET, guidance could not be performed due to suboptimal imaging. The authors point out that one of the main limitations of echocardiography is the inability to image scar, which is of key importance given the association between posterolateral wall scar and poor outcomes (7). CMR in comparison has the ability to identify and quantify both scar and dyssynchrony and may represent the optimal imaging modality for CRT guidance (6). A meta-analysis of 511 patients using STARTER, TARGET, and another prospective cohort study (20), confirmed the efficacy of an image-guided approach compared with conventional implant with a higher odds ratio of response to CRT (odds ratio: 2.1; 95% confidence interval: 1.43-3.07; $p < 0.0001$) (21).

We have previously used CMR imaging to delineate scar and dyssynchrony fused with fluoroscopy at the time of implantation (16,17). Using this technique, guided placement of the LV to CMR target segments was associated with a significantly superior hemodynamic response compared with an empirical non-targeted approach. Furthermore, 92% of the echocardiographic responders (>15% reduction in end-systolic volume) were paced in a targeted CMR target segment, compared with 50% of those who were echo nonresponders. Because of the significant time previously required for the software processing of CMR images, the scan was performed on average 2 weeks before the implant. Our current technique represents a paradigm shift, with rapid data processing, analysis, and visualization of the CMR data in the same X-MRI laboratory in a single sitting. This

FIGURE 5 **Case Example With CMR-Derived Target Segments, 3D Shell Fusion With X-Ray, and Targeted LV Lead Placement**

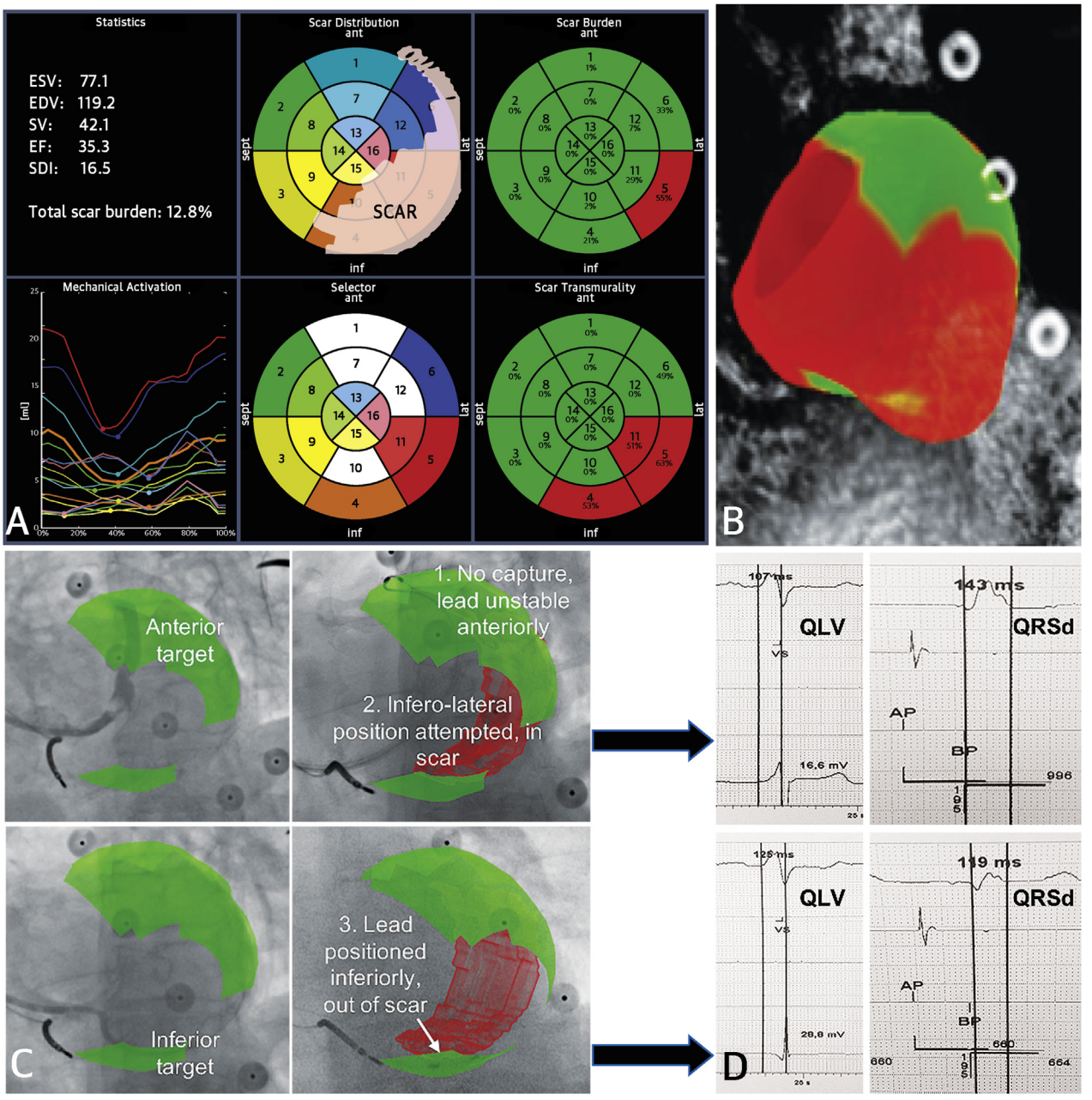

(A) Prototype guide CRT platform. Left ventricular (LV) volumes, scar burden, and dyssynchrony indices, as described in Figure 2. Myocardial scar is localized to the posterolateral region. Target segments are selected (basal and mid-anterior, mid-anterolateral, and mid-inferior). EDV = end-diastolic volume; EF = ejection fraction; ESV = end-systolic volume; SD = standard deviation; SV = stroke volume. **(B)** The CMR-derived 3D shell with selected target segments in green is demonstrated alongside the fiducial markers, as displayed through time-resolved angiography. **(C)** Left upper panel showing large anterior target segment and anterior vein. **Left lower panel** showing smaller inferior target segment and vein identified. **Right upper panel** showing the attempted positioning of LV lead in an anterior vein; however, the lead was unable to track distally and was unstable without any demonstrable biventricular capture. Subsequent positioning in a posterolateral vein (within the area of scar as shown in **red**). **Right lower panel** showing lead positioning in inferior target (poles within **green** area). **(D)** QLV (sensed electrical latency) from LV lead positioned in posterolateral vein within scar (QLV 107 ms) and biventricular paced QRS duration of 143 ms **(upper panel)**. Electrical parameters were more favorable with LV lead with poles within target area, out of scar (QLV 125 ms, paced QRS duration 119 ms) **(lower panel)**. Abbreviations as in Figure 1.

TABLE 2 Comparison of Electrical Properties Based on Whether the LV Lead Was In or Out of Areas of Scar, Determined by the CMR Overlay

	Mean Difference	95% CI	p Value
LV lead capture threshold (volts)	2.35	1.54 to 3.15	<0.001
QLV (ms)	7.78	-8.63 to 24.20	0.35
BV-paced QRS duration (ms)	24.61	15.24 to 33.97	<0.001

Mixed-effect model for all data points comparing those in and out of scar, as determined by the CMR overlay visualization using the purpose-built platform (raw data output, to 2 decimal places). A total of 56 data points were compared across 14 patients.

BV = biventricular; CI = confidence interval; QLV = first ventricular depolarization (earliest onset QRS duration on surface 12-lead electrocardiogram) to the nadir signal on the LV lead electrogram; LV = left ventricular.

process occurs in parallel with the patient being draped and central venous access being gained. Rapid image coregistration enables immediate image fusion upon CS venography allowing the implanter to perform real-time CMR-guided CRT.

Importantly, our implant times compare very favorably with previous guided CRT studies. In TARGET, implant time was 139 ± 36 min in the guidance group compared with 138 ± 42 min in the standard group (p = NS), although screening time and dose were higher in the guidance group (24 ± 14 min vs. 19 ± 13 min, p = 0.033) (9). The implant time for our patients excluding the CMR was 115 ± 33 min, despite pacing in all accessible venous sites (target and nontarget) as part of validating the system. In the future, we envisage this system being used to directly implant the target vein, likely being associated with significantly shorter implant and fluoroscopy times.

CRT OUTCOMES AND MYOCARDIAL FIBROSIS. Reported nonresponse rates to CRT are variable depending on which outcome measure is assessed but is at least 30% (3). Myocardial fibrosis, particularly in the posterolateral region where the LV lead is empirically placed, is associated with a poor response to CRT (7). Studies have described using CMR to avoid LV lead placement within scar to improve CRT response (8,22) and using multisite LV stimulation to improve hemodynamic response in this group (23). In the current study, 36% of patients had myocardial scar in the posterolateral region. Given that the majority of patients undergoing CRT have the LV lead implanted in either the lateral or posterior walls (24), it is inevitable that the lead will be in or adjacent to myocardial scar in a sizeable proportion of cases. Prior studies have highlighted the importance of both global scar burden (25) and regional scar occupying the region of the LV lead (26) on CRT outcomes. Our custom-made platform produces information regarding percentage scar burden and transmurality for each myocardial segment; this knowledge may be a useful adjunct in difficult cases with a high global scar burden by guiding the implanting physician to select those sites with the lowest segmental scar burden and transmurality. Furthermore, in cases in which LV lead placement in or adjacent to scar was inevitable because of the distribution of coronary venous anatomy, the CMR scar mask was able to guide the positioning the poles (from the multipolar LV lead) away from islands of scar to achieve more favorable testing parameters.

LIMITATIONS AND CHALLENGES. This is a small proof of principle study; however, a larger, randomized controlled study would be necessary to demonstrate whether an image-guided approach is superior to the standard of care, which we plan to perform. Given that 2 previous studies using echocardiogram-derived markers (9,10) and 2 recent studies using multimodality imaging (27,28) have all demonstrated improved clinical outcomes, this would infer that a strategy of image guidance may be of clinical benefit.

The use of CMR may not be feasible in all patients because of renal impairment and claustrophobia. Furthermore, heart failure patients especially may struggle with being supine for extended periods; therefore, this technique may not be suitable for all. Scar derivation was from routine LGE sequences in a short-axis slice format (8-mm slice, 2-mm gap), which inevitably leads to an irregularly edged mesh with gapping. Dyssynchrony was derived through endocardial wall motion tracking on routine cine imaging and volume vs. time curves used to identify segments with latest mechanical activation rather than a pure strain calculation. It could be argued that one cannot exclude passive wall motion when tracking the endocardial surface only; however, similar tracking algorithms (using cine CMR) have shown good agreement with strain derived from myocardial tagging (the gold standard for measuring strain) (29).

We anticipate future iterations of the platform to include scar analysis from LGE sequences with higher spatial resolution (higher number of slices or 3D scar) and calculation of dyssynchrony through a range of different metrics including cine sequence-derived strain, as described previously (27). In this study, of importance was that the spatial and temporal resolution were the same as for routine scanning; however, more elaborate and refined sequences may be able to be incorporated in the near future. Last, we intentionally studied a predominantly ischemic population, given that they have the most to gain

from a technique that may be able to improve CRT response. Response rates in nonischemic patients are indeed significantly higher; we would therefore advocate studying a larger number of these patients to evaluate the platform from the perspective of image guidance using dyssynchrony parameters alone.

Coronary venous anatomy has been described using 3D whole heart sequences (electrocardiogram-triggered, respiratory-navigated, steady-state free-precession inversion recovery) applied to the whole heart over a short period (e.g., 60 to 80 ms), obtaining spatial resolution of 1.5 × 1.5 × 2 mm (30). However, this process adds at least 30 min of scanning time and, furthermore, the coronary veins require segmentation to extract onto the 3D mesh model, which can be time consuming and limit the applicability of data utilization in real time. Furthermore, heart failure patients may have worsened breathing when lying supine; therefore, we wanted to keep scanning time to a minimum, before the implant, which also requires them to lie flat.

An increasing proportion of patients undergoing CRT are upgrades from existing devices and, despite the increasing availability of magnetic resonance conditional pacing systems (31), significant artifact image degradation would limit the use of a CMR-based guidance platform. We have previously shown computed tomography (CT) imaging merged with fluoroscopy can facilitate LV lead implantation in previously failed LV lead implants with visualization of CS anatomy (32). Furthermore, cardiac CT may provide a feasible alternative to CMR; measures of strain have shown to correlate between the 2 imaging modalities in an animal model (33) and scar can be demonstrated (34). We envisage using a similar guidance platform with CT data in a similar way in the future.

Given the expense of CMR in some centers, this technique may not be cost-effective; however, the data could be processed offsite and fed back to the core site. The current technique of single-sitting CMR and implant requires an X-MRI laboratory, which is not available in all centers. It is envisaged, however, that in the future, with improved image registration techniques not requiring fiducial markers, the CMR platform could be used in an offline manner with scanning and implantation in separate locations and times.

Finally, it is notable that only 71% of patients were able to have the LV lead delivered to the target segment; this is similar to our previous study of CMR guidance (15). This usually occurs from the lack of a coronary vein subtending the target segments. This may be viewed not as a limitation but as an advantage of the system. One may argue that in those cases in which the target segments are not subtended by viable epicardial veins, the conventional epicardial approach may be switched to an endocardial LV approach at the outset. Endocardial pacing has been shown to be of use in nonresponders to conventional CRT (35); however, the optimal site of stimulation varies greatly between patients (4,36,37). The value of such a system may be to both identify patients in whom such an approach is required and to then use the system to perform targeted endocardial LV lead implantation. Recently, we have shown that such a targeted approach for endocardial LV stimulation using CMR guidance to avoid scar results in improved hemodynamic response (38).

CLINICAL RELEVANCE AND FUTURE DIRECTIONS. Image guidance is likely to lead to improved response rates in patients undergoing CRT implantation. The ability of CMR to image scar as well as dyssynchrony would appear to make it the ideal clinical tool for such guidance and may result in improved responder rates. The ability to perform imaging and guidance in 1 sitting may be attractive for both the patient and clinician and may result in a more cost-effective approach to CRT. The development of LV endocardial pacing and the use of leadless pacemaker systems that can be deployed into the LV endocardium (39) are likely to be used increasingly in the future, especially in patients who are likely to respond poorly to standard CRT. Endocardial LV pacing is highly site specific, and the use of such an imaging platform to guide endocardial LV stimulation sites may be extremely important in the future.

CONCLUSIONS

Real-time CMR guidance for optimal LV lead placement in delivering CRT is safe and feasible and can be performed in a single procedure. Larger scale studies are needed to ascertain whether this process will lead to improved clinical outcome.

ACKNOWLEDGMENTS The authors acknowledge Drs. Manav Sohal and Shaumik Adhya, who implanted patients using the software platform. The authors also acknowledge Professor Janet Peacock, head of Medical Statistics, King's College London, for statistics support. The methods presented in this paper are based on research and are not commercially available.

ADDRESS FOR CORRESPONDENCE: Dr. Jonathan M. Behar, c/o Imaging Sciences & Biomedical Engineering, 4th Floor Lambeth Wing, St Thomas' Hospital, Westminster Bridge Road, London SE1 7EH, United Kingdom. E-mail: jonathanbehar@gmail.com.

PERSPECTIVES

COMPETENCY IN MEDICAL KNOWLEDGE: Implantation of CRT using a CMR-derived image guidance platform is feasible and, furthermore, targeted LV lead delivery in myocardial regions that are out of scar and dyssynchronous may improve CRT outcomes.

TRANSLATIONAL OUTLOOK: Given the recent interest and enthusiasm for LV endocardial stimulation and wireless pacing to deliver CRT, this technology and technique may be a highly valuable adjunct for implanting physicians.

REFERENCES

1. Cleland JGF, Daubert J-C, Erdmann E, et al. The effect of cardiac resynchronization on morbidity and mortality in heart failure. N Engl J Med 2005;352:1539–49.

2. Bristow MR, Saxon LA, Boehmer J, et al. Cardiac-resynchronization therapy with or without an implantable defibrillator in advanced chronic heart failure. N Engl J Med 2004;350:2140–50.

3. Daubert J-C, Saxon L, Adamson PB, et al. 2012 EHRA/HRS expert consensus statement on cardiac resynchronization therapy in heart failure: implant and follow-up recommendations and management. Europace 2012;14:1236–86.

4. Derval N, Steendijk P, Gula LJ, et al. Optimizing hemodynamics in heart failure patients by systematic screening of left ventricular pacing sites: the lateral left ventricular wall and the coronary sinus are rarely the best sites. J Am Coll Cardiol 2010;55:566–75.

5. Mullens W, Verga T, Grimm RA, Starling RC, Wilkoff BL, Tang WHW. Persistent hemodynamic benefits of cardiac resynchronization therapy with disease progression in advanced heart failure. J Am Coll Cardiol 2009;53:600–7.

6. Leyva F. Cardiac resynchronization therapy guided by cardiovascular magnetic resonance. J Cardiovasc Magn Reson 2010;12:64.

7. Bleeker GB, Kaandorp TAM, Lamb HJ, et al. Effect of posterolateral scar tissue on clinical and echocardiographic improvement after cardiac resynchronization therapy. Circulation 2006;113:969–76.

8. Ginks MR, Lambiase PD, Duckett SG, et al. A simultaneous x-ray/MRI and noncontact mapping study of the acute hemodynamic effect of left ventricular endocardial and epicardial cardiac resynchronization therapy in humans. Circ Heart Fail 2011;4:170–9.

9. Khan FZ, Virdee MS, Palmer CR, et al. Targeted left ventricular lead placement to guide cardiac resynchronization therapy: the TARGET study: a randomized, controlled trial. J Am Coll Cardiol 2012;59:1509–18.

10. Saba S, Marek J, Schwartzman D, et al. Echocardiography-guided left ventricular lead placement for cardiac resynchronization therapy: results of the Speckle Tracking Assisted Resynchronization Therapy for Electrode Region trial. Circ Heart Fail 2013;6:427–34.

11. Yu C-M, Bax JJ, Gorcsan J. Critical appraisal of methods to assess mechanical dyssynchrony. Curr Opin Cardiol 2009;24:18–28.

12. Bax JJ, Gorcsan J. Echocardiography and noninvasive imaging in cardiac resynchronization therapy: results of the PROSPECT (Predictors of Response to Cardiac Resynchronization Therapy) study in perspective. J Am Coll Cardiol 2009;53:1933–43.

13. Simonetti OP, Kim RJ, Fieno DS, et al. An improved MR imaging technique for the visualization of myocardial infarction. Radiology 2001;218:215–23.

14. Chalil S, Stegemann B, Muhyaldeen S, et al. Intraventricular dyssynchrony predicts mortality and morbidity after cardiac resynchronization therapy : a study using cardiovascular magnetic resonance tissue synchronization imaging. J Am Coll Cardiol 2007;50:243–52.

15. Sohal M, Shetty A, Duckett S, et al. Noninvasive assessment of LV contraction patterns using CMR to identify responders to CRT. J Am Coll Cardiol Cardiol Img 2013;6:864–73.

16. Shetty AK, Duckett SG, Ginks MR, et al. Cardiac magnetic resonance-derived anatomy, scar, and dyssynchrony fused with fluoroscopy to guide LV lead placement in cardiac resynchronization therapy: a comparison with acute haemodynamic measures and echocardiographic reverse remodelling. Eur Heart J Cardiovasc Imaging 2013;14:692–9.

17. Duckett SG, Ginks M, Knowles BR, et al. A novel cardiac MRI protocol to guide successful cardiac resynchronization therapy implantation. Circ Heart Fail 2010;3:e18–21.

18. Jolly M-P, Guetter C, Lu X, Xue H, Guehring J. Automatic segmentation of the myocardium in cine MR images using deformable registration. In: Camera O, Konukoglu E, Pop M, et al., editors. Statistical Atlases and Computational Models of the Heart. Imaging and Modelling Challenges. Berlin: Springer, 2012:98–108.

19. Khan FZ, Virdee MS, Read PA, et al. Effect of low-amplitude two-dimensional radial strain at left ventricular pacing sites on response to cardiac resynchronization therapy. J Am Soc Echocardiogr 2010;23:1168–76.

20. Bai R, Di Biase L, Mohanty P, et al. Positioning of left ventricular pacing lead guided by intracardiac echocardiography with vector velocity imaging during cardiac resynchronization therapy procedure. J Cardiovasc Electrophysiol 2011;22:1034–41.

21. Jin Y, Zhang Q, Mao J-L, He B. Image-guided left ventricular lead placement in cardiac resynchronization therapy for patients with heart failure: a meta-analysis. BMC Cardiovasc Disord 2015;15:36.

22. Leyva F, Foley PWX, Chalil S, et al. Cardiac resynchronization therapy guided by late gadolinium-enhancement cardiovascular magnetic resonance. J Cardiovasc Magn Reson 2011;13:29.

23. Ginks MR, Duckett SG, Kapetanakis S, et al. Multi-site left ventricular pacing as a potential treatment for patients with postero-lateral scar: insights from cardiac magnetic resonance imaging and invasive haemodynamic assessment. Europace 2012;14:373–9.

24. Singh JP, Klein HU, Huang DT, et al. Left ventricular lead position and clinical outcome in the multicenter automatic defibrillator implantation trial-cardiac resynchronization therapy (MADIT-CRT) trial. Circulation 2011;123:1159–66.

25. Ypenburg C, Roes SD, Bleeker GB, et al. Effect of total scar burden on contrast-enhanced magnetic resonance imaging on response to cardiac resynchronization therapy. Am J Cardiol 2007;99:657–60.

26. Wong JA, Yee R, Stirrat J, et al. Influence of pacing site characteristics on response to cardiac resynchronization therapy. Circ Cardiovasc Imaging 2013;6:542–50.

27. Bertini M, Mele D, Malagù M, et al. Cardiac resynchronization therapy guided by multimodality cardiac imaging. Eur J HeartFail 2016;18:1375–82.

28. Sommer A, Kronborg MB, Nørgaard BL, et al. Multimodality imaging-guided left ventricular lead placement in cardiac resynchronization therapy: a randomized controlled trial. Eur J Heart Fail 2016;18:1365–74.

29. Moody WE, Taylor RJ, Edwards NC, et al. Comparison of magnetic resonance feature tracking for systolic and diastolic strain and strain rate calculation with spatial modulation of magnetization imaging analysis. J Magn Reson Imaging 2015;41:1000–12.

30. Duckett SG, Chiribiri A, Ginks MR, et al. Cardiac MRI to investigate myocardial scar and coronary venous anatomy using a slow infusion of dimeglumine gadobenate in patients

undergoing assessment for cardiac resynchronization therapy. J Magn Reson Imaging 2011;33:87–95.

31. Lowe MD, Plummer CJ, Manisty CH, Linker NJ. Safe use of MRI in people with cardiac implantable electronic devices: Figure 1. Heart 2015;101:1950–3.

32. Duckett SG, Ginks MR, Knowles BR, et al. Advanced Image fusion to overlay coronary sinus anatomy with real-time fluoroscopy to facilitate left ventricular lead implantation in CRT. Pacing Clin Electrophysiol 2011;34:226–34.

33. Pourmorteza A, Schuleri KH, Herzka DA, Lardo AC, McVeigh ER. A new method for cardiac computed tomography regional function assessment: stretch quantifier for endocardial engraved zones (SQUEEZ). Circ Cardiovasc Imaging 2012;5:243–50.

34. Jeevarethinam A, Venuraju S, Mehta VS, et al. Myocardial scar detection by standard CT coronary angiography. Cardiol Res 2014;5:118–20.

35. Morgan JM, Biffi M, Geller LA, et al. Feasibility and safety results of a novel superior-access, atrial transseptal approach to left ventricular endocardial lead implantation: one month follow-up of the alternate site cardiac resynchronization (ALSYNC) study. Heart Rhythm 2014;11:S40–1.

36. Spragg DD, Dong J, Fetics BJ, et al. Optimal left ventricular endocardial pacing sites for cardiac resynchronization therapy in patients with ischemic cardiomyopathy. J Am Coll Cardiol 2010;56:774–81.

37. Shetty AK, Sohal M, Chen Z, et al. A comparison of left ventricular endocardial, multisite, and multipolar epicardial cardiac resynchronization: an acute haemodynamic and electroanatomical study. Europace 2014;16:873–9.

38. Behar JM, Jackson T, Hyde E, et al. Optimised left ventricular endocardial stimulation is superior to optimised epicardial stimulation in ischemic patients with poor CRT response: a combined magnetic resonance imaging, electro-anatomical contact mapping and hemodynamic study to target endocardial lead placement. J Am Coll Cardiol EP 2016;2:799–809.

39. Auricchio A, Delnoy PP, Butter C, et al. Feasibility, safety, and short-term outcome of leadless ultrasound-based endocardial left ventricular resynchronization in heart failure patients: results of the Wireless Stimulation Endocardially for CRT (WiSE-CRT) study. Europace 2014;16:681–8.

KEY WORDS cardiac magnetic resonance (CMR), cardiac resynchronization therapy (CRT) image guidance, image overlay, targeted LV lead placement

APPENDIX For a supplemental table, please see the online version of this article.